

## Laboratory experiments for exploring the surface plasmon resonance

This article has been downloaded from IOPscience. Please scroll down to see the full text article.

2011 Eur. J. Phys. 32 585

(<http://iopscience.iop.org/0143-0807/32/2/028>)

View [the table of contents for this issue](#), or go to the [journal homepage](#) for more

Download details:

IP Address: 81.57.241.117

The article was downloaded on 19/02/2011 at 10:13

Please note that [terms and conditions apply](#).

# Laboratory experiments for exploring the surface plasmon resonance

Olivier Pluchery<sup>1</sup>, Romain Vayron and Kha-Man Van

Institut des NanoSciences de Paris, Université Pierre et Marie Curie UPMC-CNRS,  
4 place Jussieu, 75005 Paris, France

E-mail: [olivier.pluchery@insp.jussieu.fr](mailto:olivier.pluchery@insp.jussieu.fr)

Received 3 November 2010, in final form 22 December 2010

Published 18 February 2011

Online at [stacks.iop.org/EJP/32/585](http://stacks.iop.org/EJP/32/585)

## Abstract

The surface plasmon wave is a surface wave confined at the interface between a dielectric and a metal. The excitation of the surface plasmon resonance (SPR) on a gold thin film is discussed within the Kretschmann configuration, where the coupling with the excitation light is achieved by means of a prism in total reflection. The electromagnetic principles are detailed and a simple experimental setup is described that can be used for laboratory experiments for senior students in the third or fourth year of university. This experiment allows accurate determination of the angle of plasmon extinction and discussion of the principles of biosensors based on the SPR. A slight modification of the setup allows the investigation of the dependence of SPR on wavelength and illustrates the damping of SPR due to its coupling with the interband transitions of the gold thin film.

(Some figures in this article are in colour only in the electronic version)

## 1. Introduction

The surface plasmon resonance (SPR) corresponds to a coherent oscillation of electrons that takes place at the interface between a metal and a dielectric medium. The coupling with an electromagnetic wave gives rise to a confined surface wave and very particular optical properties. The first observation of such a plasmon wave was made by A Otto in 1968 [1] and the experimental setup was improved by E Kretschmann [2]. Since then, the properties of SPR have been thoroughly studied, giving birth to a specific research field called plasmonics, and many developments have been conducted for the design of commercial apparatus for biophysics (Biacore<sup>®</sup> in 1990 followed by many others). This paper presents a laboratory experiment that explores the main SPR properties from the point of view of electromagnetism. It provides a good way for producing surface waves that are confined in subwavelength scales

<sup>1</sup> Author to whom any correspondence should be addressed.

and can serve as an introduction to nano-optics. It demonstrates the incredible sensitivity of SPR to surface phenomena and can be further developed towards biosensing. The experiment is based on inexpensive optical equipment and has been used in different physics courses. It is currently proposed to senior students in their fourth year at the Ecole Normale Supérieure de Cachan (France) as a 1 week project. Within a limited time of 4 full days, a group of three students has to get familiar with the concepts of SPR, set up the experiment, collect data and check them against theoretical predictions. This project is organized within the Optics Laboratory of the University and the students can ask for any available equipment to improve the experiment. It is also proposed as regular laboratory experiments that can be completed within 4 h. In this configuration, the setup is already prepared when students start working.

The paper first presents the basics of SPR, and then describes the experimental setup and the results. The last part discusses three other experiments that can be conducted with the setup.

## 2. Theoretical considerations regarding the SPR

This part summarizes the content of an introductory lesson taught to the students. Plasmon resonance is usually not part of their current courses although they already have the conceptual tools to understand it. The main steps of the derivation are given in the body of the text and a complete derivation of the SPR main formula is added in the appendix or can be found in many textbooks [3, 4]. The SI unit system is used.

### 2.1. Electron oscillation

In the case of a metal, the bulk free electrons can oscillate with an eigenfrequency given by the plasma frequency  $\omega_p^2 = \frac{ne^2}{\epsilon_0 m}$  with energies close to 10 eV. However close to the metallic surface this oscillation occurs with a lower energy and gives rise to a longitudinal charge density wave propagating along the interface [5]. This density wave is called a plasmon polariton. The coupling of this electron oscillation with the electromagnetic field is the most straightforward way to detect this wave and the resulting optical wave is the surface plasmon (SP) wave. The mechanical wave (oscillation of charges) and the optical wave (oscillation of the electric field) are inextricably coupled, and this explains why their names are sometimes mixed up. In this paper we will deal with the optical aspect of the phenomenon. In the case of gold or silver this coupling occurs in the visible range and can be seen with the naked eye. Note that the SPR is not identical to the localized plasmon resonance which is often abusively called localized *surface* plasmon resonance (LSPR). The latter takes place in small metallic particles and corresponds to a global oscillation of the charges (plasma oscillation) constrained by the tight boundary conditions imposed by the spheroidal shape of the particles.

### 2.2. Evanescent waves and surfaces waves

Since the SPR is a surface wave, we shortly discuss the structure of this kind of wave. The coupling of this wave with the dielectric medium at the other side of the interface will be considered in the next section. Let us consider the propagation of the electric field in a metallic medium of dielectric function  $\epsilon_1(\omega)$  close to an interface defined by  $z = 0$  (see figure 1). We seek solutions in the form of plane waves written as  $\vec{E}_1(\vec{r}, \omega) = \vec{E}_0 e^{i(\vec{k}\cdot\vec{r} - \omega t)}$ . They obey the differential wave equation given by

$$\nabla^2 \vec{E}_1(\vec{r}, \omega) + \epsilon_1(\omega) \frac{\omega^2}{c^2} \vec{E}_1(\vec{r}, \omega) = 0 \quad (1)$$

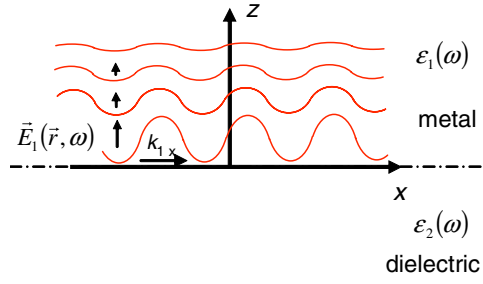


**Figure 1.** Structure of a surface wave (evanescent wave). The wave propagates along the  $x$  direction with a wavevector  $k_{1x}$  and has an exponentially vanishing amplitude in the direction normal to the interface (direction  $z$ ). In the  $z$  direction the decay length is given by  $1/k_z$  and there is no propagation but an oscillation of the electric field as a whole.

and the dispersion equation which rules the propagation of the plane wave:

$$-k_1^2 + \varepsilon_1(\omega) \frac{\omega^2}{c^2} = 0. \quad (2)$$

By choosing the orientation of the axis such that  $\vec{k}_1 = k_{1x}\vec{u}_x + k_{1z}\vec{u}_z$ , relation (2) becomes

$$k_{1x}^2 + k_{1z}^2 = \varepsilon_1(\omega) \frac{\omega^2}{c^2}. \quad (3)$$

The dielectric function  $\varepsilon_1(\omega)$  of a metal is predominantly a real number with a negative value. Hence, in order to fulfil relation (3), either  $k_{1x}$  or  $k_{1z}$  should be an imaginary number. The aim of the derivation is to find expressions for the wavevectors  $k_{1x}$  and  $k_{1z}$  at a given angular frequency  $\omega$ . This will be achieved in the next section, but before that we discuss the structure of the resulting wave. Let us assume the following expressions for the wavevector:

$$\begin{aligned} k_{1x} &= k'_{1x} \\ k_{1z} &= ik''_{1z}. \end{aligned} \quad (4)$$

Then the resulting wave is an evanescent wave [3] or surface wave given by

$$\vec{E}_1(\vec{r}, \omega) = \vec{E}_0 e^{-k''_{1z}z} e^{i(k'_{1x}x - \omega t)}. \quad (5)$$

This wave is propagating along the  $x$  direction and has exponentially decreasing amplitude along the  $z$  direction as illustrated in figure 1. The  $1/e$  decay length is given by  $1/k_{1z}$  ( $1/2 \cdot k_{1z}$  for the intensity) so that the wave is confined on the surface at a distance of approximately  $1/k_{1z}$ . The SP wave is a wave of this kind and the typical confinement thickness in the metal is of the order of 30 nm (in gold at a wavelength of 633 nm). Note that in the actual plasmon wave,  $k_{1x}$  has a nonzero imaginary part ( $k_{1x} = k'_{1x} + ik''_{1x}$ ), so that the surface wave is damped along the  $x$  direction as well. The typical decay length in this direction is 10  $\mu\text{m}$  (gold film at a wavelength of 633 nm), so that such a wave will not go very far on gold interfaces.

### 2.3. The SP wave

The optical evanescent wave discussed above is intrinsically coupled to a second evanescent wave on the dielectric side of the interface, and this coupling results in the SP wave. As a consequence, any change in the dielectric medium close to the interface that affects the optical

index will modify the propagation of the plasmon wave. In this section, we give details of the relations needed to accurately describe the SP wave. Medium 1 is homogeneous, isotropic and metallic with dielectric function  $\varepsilon_1(\omega)$  and has a plane interface at  $z = 0$  with medium 2 which is a homogeneous and isotropic dielectric. The dielectric function  $\varepsilon_2(\omega)$  is a real and positive function. As far as metal is concerned, we will consider gold whose dielectric function can be crudely approximated with the Drude–Sommerfeld model that takes into account the free electrons of the metal. In that approach,  $\varepsilon_1(\omega)$  is given by

$$\varepsilon_{1 \text{ Drude}} = 1 - \frac{\omega_p^2}{\omega^2 - i\Gamma\omega} \approx 1 - \frac{\omega_p^2}{\omega^2} \quad \text{with} \quad (6)$$

$$\begin{cases} \hbar\omega_p = 8.95 \text{ eV, i.e. } \omega_p = 1.36 \times 10^{16} \text{ rad s}^{-1} \\ \hbar\Gamma = 65.8 \text{ meV, i.e. } \Gamma = 1.0 \times 10^{14} \text{ rad s}^{-1}. \end{cases}$$

As soon as  $\omega$  is smaller than  $\omega_p$ , the real part of  $\varepsilon_1(\omega)$  becomes negative with values around  $-10$  for electromagnetic waves in the visible range. This Drude model helps one to obtain the global trend, but precise experimental values are needed for a satisfactory match between calculations and measurements [6–8].

We now look for an eigenmode of the wave equation (1) in both media, compatible with the boundary conditions imposed by the plane interface (see the appendix for more details). Only waves with their electric field polarized within the plane of incidence (polarization  $p$ , see figure 3) are solutions and the electric fields in media 1 and 2 are surface waves characterized by decay lengths and  $1/k_{1z}$ ,  $1/k_{2z}$  and a wavevector parallel to the interface which has equal values for the two waves  $k_{1x} = k_{2x} = k_x$ .

From the dispersion equations written in each of the two media, and from the boundary conditions applied to the electric field  $\vec{E}$  and electric displacement  $\vec{D}$ , the dispersion equation of the SP wave is derived and written as

$$k_x^2 = \frac{\omega^2}{c^2} \cdot \frac{\varepsilon_1(\omega) \cdot \varepsilon_2(\omega)}{\varepsilon_1(\omega) + \varepsilon_2(\omega)} \quad (7)$$

$$k_{1z}^2 = \frac{\omega^2}{c^2} \cdot \frac{\varepsilon_1^2(\omega)}{\varepsilon_1(\omega) + \varepsilon_2(\omega)} \quad \text{and} \quad k_{2z}^2 = \frac{\omega^2}{c^2} \cdot \frac{\varepsilon_2^2(\omega)}{\varepsilon_1(\omega) + \varepsilon_2(\omega)}. \quad (8)$$

Relation (7) is the fundamental expression to derive the main properties of SPR. Note that at the interface between metallic and dielectric media, expression (7) is likely to be positive since  $\varepsilon_1$  is around  $-10$  (imaginary part of  $\varepsilon_1$  neglected in a first approximation) and  $\varepsilon_2 = 1$  if medium 2 is air. It gives rise to a real  $k_x$  wavevector as anticipated in section 2.2 and therefore a propagation along the interface. From relation (8) one can also check that  $k_{1z}^2$  and  $k_{2z}^2$  are negative, so that the components of the wavevectors perpendicular to the interface are imaginary numbers. This confirms that the resulting wave is evanescent in the direction away from interface, both in the metal (gold) and in air with decay lengths calculated at 30 and 370 nm respectively. Such a confinement demonstrates that the SP wave is a surface wave.

#### 2.4. Excitation of the SP wave

The SP wave is an eigenmode of a surface wave and the most popular way of exciting it is the coupling to an external optical beam. The coupling of two electromagnetic waves requires the conservation of both the energy  $\hbar\omega$  and the momentum  $\hbar\vec{k}$  of the excitation wave. The plot of the angular frequency  $\omega$  as a function of the wavevector is the best way to visualize the conditions where these two conservation laws are fulfilled. By plotting simultaneously the dispersion relations of the SP wave and the excitation wave, it is easy to determine

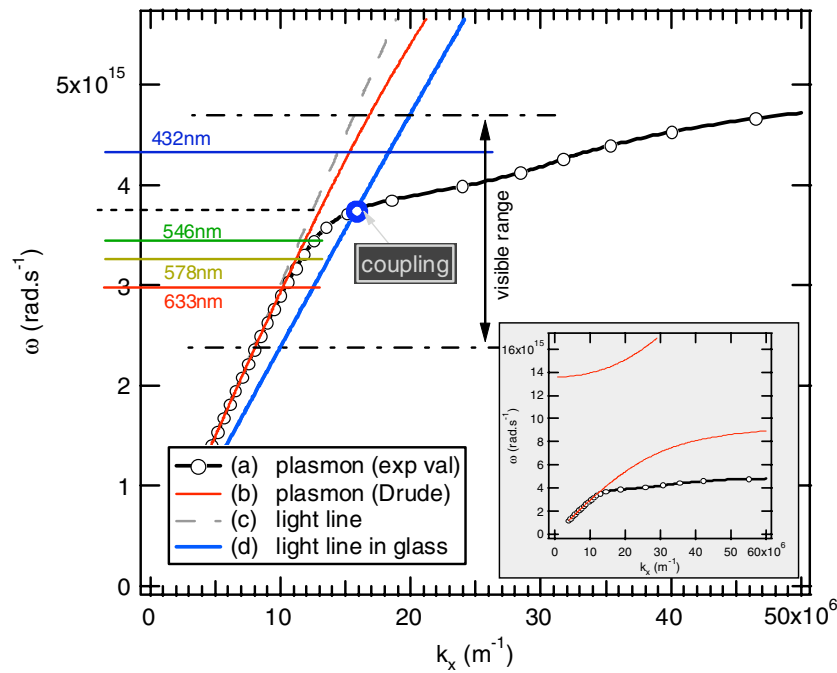


**Figure 2.** Dispersion relation of the surface plasmon wave at a gold/air interface. Curves (a) and (b) are the plots of the dispersion relation (7) given in the text. Curve (a) is obtained using the experimental values for the dielectric function of gold [6], whereas curve (b) is based on the Drude model (see relation (6) in the text) that does not take into account the contribution from the interband transitions of gold. Line (c) is the light line, which represents the dispersion relation of a beam impinging directly on the metallic surface. The absence of intersection between lines (a) and (c) shows that the coupling of the SP wave with such an external wave is not possible. Line (d) corresponds to the dispersion relation of a wave going through a glass prism with an angle of  $60^\circ$  with respect to the interface. The inset presents the plots of the plasmon dispersion relations (a) and (b) over a larger range showing the deviation from the free-electron model and illustrating strong influence of the bound electrons (interband transitions) in the case of gold.

whether the two curves cross and the conditions that ensure this intersection. Figure 2 is a plot of the dispersion equation of the SP wave and its coupling with an excitation wave in the case of a gold/air interface. On this graph two dispersion relations for the SP wave are represented according to equation (7): line (a) corresponds to the most accurate plot based on the experimental values for the dielectric function of gold [6] and line (b) uses the simple Drude model from equation (6) that only takes into account the free electrons of the metal. The strong differences between the two plots show that the electronic properties of gold cannot be satisfactorily described by the free electrons only. Therefore the following discussion will be based on the more realistic relation (a).

Let us consider an external wave propagating in air (medium 2, wavevector  $\vec{k}_2$ ) impinging on the metallic surface with an incidence angle  $\theta$  (see figure 3). The component of the wavevector parallel to the interface  $k_{2x} = k_x$  obeys the dispersion relation  $\omega = \frac{k_x \cdot c}{\sin \theta}$  which is represented by the light line (c) on figure 2 in the case  $\theta = \pi/2$ . As evidenced by the graph, this light never crosses the SP dispersion relation. For an incidence angle smaller than  $\pi/2$ , the slope of the light line is even greater and the intersection of any of the light lines with the SP dispersion relation never occurs. Therefore, this graph shows that an external excitation

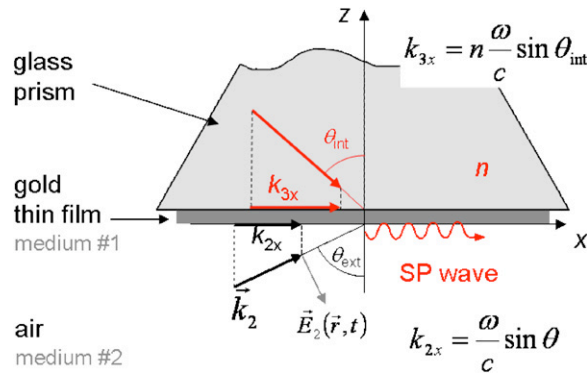


**Figure 3.** Sketch of impinging waves on a metallic film for exciting the SP wave in the Kretschmann configuration. The wave of the wave vector  $\vec{k}_3$  travels through the glass prism and creates a wavevector component  $k_{3x}$  large enough to excite the SP wave which is launched at the gold/air interface. The wave of the wavevector  $\vec{k}_2$  is unable to couple with the SP wave. This coupling only occurs for *p*-polarized waves (electric field within the plane of incidence which in our case coincides with the plane of the figure).

always yields  $k_x$  values too small to couple with the SP wave. One method to produce larger  $k_x$  is to launch a wave inside a medium of optical index  $n$  with an incidence angle greater than the critical angle. This third medium is often a glass prism. The wave is totally reflected and generates an evanescent wave on the other side of the interface (in the gold medium in figure 3). If  $\theta_{\text{int}}$  is the incidence angle as depicted on figure 3, the dispersion relation is written as

$$\begin{aligned} \omega &= \frac{k_{3x} \cdot c}{n \cdot \sin \theta_{\text{int}}} \\ &= \frac{k_x \cdot c}{n \cdot \sin \theta_{\text{int}}}. \end{aligned} \quad (9)$$

Since  $n > 1$ , the slope of this light line in the  $\omega(k_x)$  graph is lowered and the coupling between this wave and the SP wave is possible, as marked on figure 2.

Since the transfer of the momentum  $\hbar k_x$  from the glass/gold interface to the gold/air interface occurs through the gold thin film, its thickness is critical. If the gold film is too thick, the energy of this evanescent wave is absorbed and the coupling is poor. Inside the gold thin film, the electromagnetic wave undergoes multiple reflections, and this can maximize the transfer of the momentum  $\hbar k_x$  through the film thanks to constructive interferences. Therefore if the film is too thin, no constructive interference takes place and the SP wave is weakly excited. An optimal thickness, which depends on the exciting wavelength, is required to maximize the momentum transfer. This way of exciting the SP wave is called the Kretschmann configuration and is the easiest to achieve. Another way is the Otto configuration where the metallic surface is positioned away from the prism surface but close enough to capture the evanescent wave generated at a glass/air interface [1].

Therefore the condition for coupling the excitation wave with the SP wave is obtained by combining relations (7) and (9):

$$(n \sin \theta_{\text{int}})^2 = \frac{\varepsilon_1(\omega) \cdot \varepsilon_2(\omega)}{\varepsilon_1(\omega) + \varepsilon_2(\omega)}. \quad (10)$$

Note that in the case of the gold/air interface,  $\varepsilon_2 = 1$ , but this formula is written in more general cases where medium 2 is a dielectric medium such as a liquid or a molecular layer

adsorbed on the gold surface. Relation (10) is the fundamental equation that defines the conditions for SPR to occur. Practically, the exciting wave is generated by a laser beam with a given angular frequency  $\omega$ . In figure 2, this defines a point on the SP dispersion relation. The incidence angle of this laser beam  $\theta_{\text{int}}$  has to be adjusted so that the light line given by relation (9) goes through this point. This angle is a solution of equation (10). When this condition is fulfilled, the energy of the incident wave is converted into the SP wave and the reflected beam is damped. This is the plasmon extinction which is the usual way to detect the SPR.

### 3. Inexpensive experimental setup for detecting the SPR

The core of the experiment is the measurement of the plasmon extinction described in the previous section. This requires a few optical elements that can be mounted on common optical benches. Their principal characteristics are detailed below.

#### 3.1. Light source

The light source should be monochromatic and  $p$ -polarized. A polarized He–Ne laser ( $\lambda = 632.8$  nm) with 5 mW average power is well suited to this experiment. For some experiments, it is useful to use a beam expander to enlarge the laser beam and produce a convergent beam (see section 5.1 and figure 6). A beam expander can be realized with a microscope objective ( $\times 60$ , for example) and a calibrated aperture ( $50 \mu\text{m}$ ). The addition of a half-wave plate is practical because it allows changing the polarization from  $p$  to  $s$  and is a way for turning on and off the SPR. The use of an unpolarized He–Ne laser followed by a linear polarizer may cause some trouble because many lasers use to randomly switch between different modes of different polarization states and the light intensity after the polarizer becomes unstable. Another solution consists in replacing the laser with a white lamp with an interferential filter and a polarizer. The filter should have a narrow bandwidth of less than 3 nm. The resulting energy may be very low on the detector and makes accurate measurement difficult. However this solution offers the possibility of tuning the excitation wavelength by changing the filter (see section 5.2).

#### 3.2. The prism and the gold thin film

A high-index equilateral prism is used ( $n = 1.601 \pm 0.007$  for  $\lambda = 632.8$  nm). Instead of depositing a thin film of gold [9], SPR glass slides were bought from commercial vendors and adapted on one side of the prism with an index matching liquid. This solution has the advantage of using optimized gold thin films and allows one to replace the gold surface when it is damaged. The thickness of the gold thin film is critical and in the case of a SP wave at the gold/air interface excited at  $\lambda = 632.8$  nm, the thickness that ensures 100% coupling is 50 nm. With an error of 10 nm in gold thickness, the coupling decreases to 93% (40 nm) or 83% (60 nm) and if the gold layer is 100 nm thick the coupling drops to 9% (calculated values).

#### 3.3. Rotation stage

A manual rotation stage with an accuracy of  $0.1^\circ$  is used for measuring the angle  $\theta_{\text{ext}}$  defined in figure 4. The prism is positioned on the stage so that the  $180^\circ$  angle corresponds to the laser beam being back reflected to the laser. This allows us to directly measure the angle marked  $\theta_{\text{ext}}$  in figure 4(b). The value of  $\theta_{\text{int}}$  of relation (10) is obtained by the following relation,



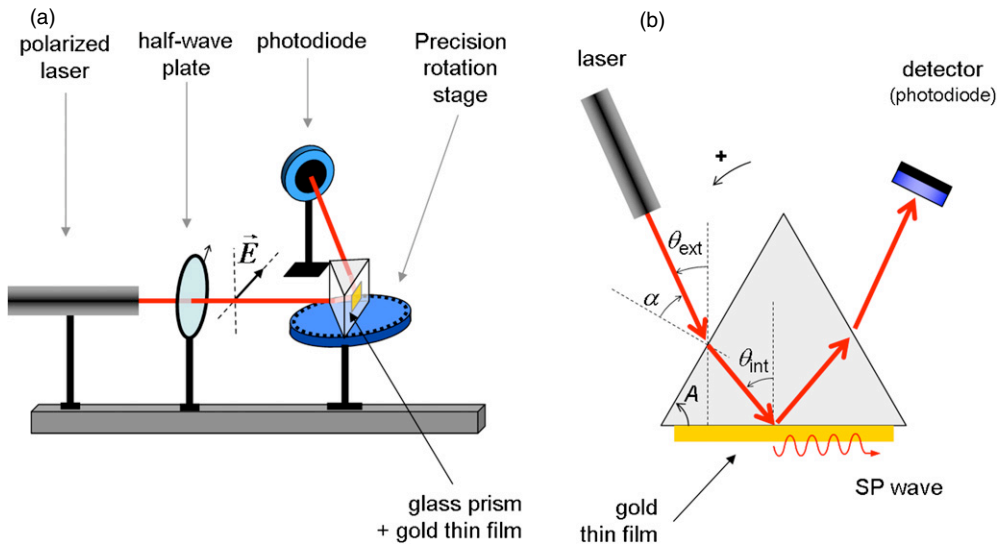


**Figure 4.** Optical setup for measuring the plasmon extinction. Monochromatic  $p$ -polarized light impinges on a prism in a total reflection configuration. An ultrathin gold film (thickness 50 nm) is placed on the prism so that it collects the evanescent waves produced by the total reflection and the SP wave is launched at the gold/air interface if the angle is set at a given value. The light intensity reflected by the prism is measured with the photodiode and goes through a minimum when the coupling with the plasmon wave occurs.

where the angles are oriented according to the counter-clockwise orientation of the plane as indicated in figure 4(b):

$$\theta_{int} = \arcsin \frac{\sin(\theta_{ext} - A)}{n} + A. \quad (11)$$

Angle  $A$  is the angle of the prism indicated in figure 4(b) and has been precisely measured at  $+59.99^\circ$  in our case. It is important to note that the measurement of the deviation angle defined by the angle between the incident laser beam and the detected beam is very inaccurate although this may be the first natural idea. Such a method assumes that both beams cross exactly above the axis of the rotation stage. This can be achieved for one angle only, and varies when rotating the stage because of the refraction of the incident beam at the prism surface.

### 3.4. Detection

The reflected beam is collected with a reversed biased photodiode and its intensity can be read with a multimeter. A resistance of 20 k $\Omega$  is used to read the voltage and the photodiode is chosen so that the sensor area is greater than the section of the laser beam. The detector is moved manually for each value of the angle.

## 4. Results and discussion

Figure 5 presents the results obtained with this setup. The reflected intensity measured with the photodiode has been recorded manually as a function of the external angle  $\theta_{ext}$  (angle defined in figure 4(b)). These raw data are plotted in the inset of figure 5. But the relevant variable for plotting the evolution of the reflected intensity is defined by equation (10) and is

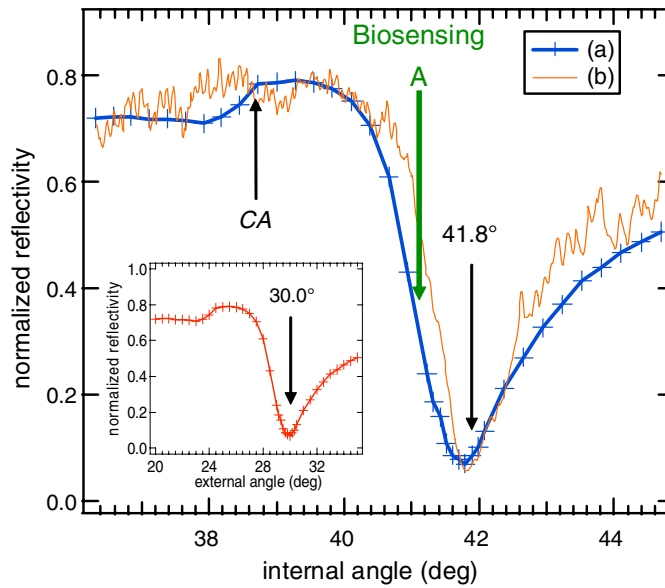


**Figure 5.** Surface plasmon extinction curve for a gold/air interface measured at a wavelength of 632.8 nm. The inset shows the normalized reflected intensity as a function of the external angle  $\theta_{\text{ext}}$  and the main graph shows the same intensity plotted versus  $\theta_{\text{int}}$  as obtained with relation (11). The intensities are normalized with the intensity of the incident laser beam. The SPR is measured at  $41.8^\circ$ . The break marked CA corresponds to the critical angle for total internal reflection. The angle marked A is a good angular position for monitoring the chemical modification of the surface due to biointeraction, for example.

the internal angle  $\theta_{\text{int}}$ . It is given by formula (11). The signature of the plasmon excitation is the sharp dip in the reflection curve around  $\theta_{\text{int}} = \theta_{\text{plasmon}} = 41.8 \pm 0.1^\circ$ . The intensity almost drops to zero which is the sign that the excitation beam transfers its energy to the SP wave. The width at half maximum of this SPR is around  $1.5^\circ$ . Since the SP wave is a surface wave confined in a 300 nm thick air layer, it cannot be detected directly except with a scanning near-field optical microscope (SNOM) that could collect the plasmon wave. But this technique is not easily accessible for laboratory experiments. Nevertheless if the surface of the gold film is damaged or exhibits some roughness, the near-field of the surface wave is converted into far-field propagating waves and causes diffusion. In this case the coupling with the plasmon wave can be visualized when the gold surface starts to glow. The angular position of the SPR is extremely dependent on the quality and the cleanliness of the gold surface. This property makes the SPR highly suitable for biosensors; however, in the case of laboratory experiments such sensitivity leads to a poor reproducibility. For example, similar measurements conducted with another gold slide that was polluted with organic molecules yields  $\theta_{\text{plasmon}} = 41.4^\circ$ .

The reflectivity curve displays a break marked CA in figure 5 which corresponds to the critical angle of total internal reflection given by  $\arcsin 1/n$ . For an angle larger than the CA, the excitation beam is fully reflected on the internal interface of the prism, which creates the evanescent wave needed to excite the SP wave as discussed in section 2. It is crucial that this total internal reflection occurs on the interface with the gold thin film, which may not always happen when using an index matching liquid (if the total reflection occurs at the prism/index liquid interface, the plasmon is not excited).

The measured value of  $\theta_{\text{plasmon}}$  at which the SPR occurs can be used to estimate the dielectric function of gold, using relation (10). The measure presented here yields  $\epsilon_{\text{Au}} = -8.1 \pm 0.9$  at 632.8 nm which has to be compared with the experimental value of  $-11.2$  [8]. The discrepancy is due again to the fact that the measurements are performed in air and the gold surface is probably covered by various contaminants. Actually, a water layer on clean gold of no more than 3 nm will cause a shift of the plasmon resonance of  $+0.2^\circ$  [3].

On the other hand, the exact calculation of the reflected intensity as a function of the internal angle reproducing the plasmon extinction is possible. It can be achieved with the Fresnel relations applied in a three-layer model. The crucial part is to implement a calculation based on the complex dielectric function of gold. The shape presented in the experimental results in figure 5 is almost exactly reproduced to the extent that the proper values for the dielectric function of gold have been used. Very often, gold left at room atmosphere is covered with contaminants or at least with a few layers of water, which is enough to shift the plasmon extinction.

## 5. Complementary experiments with the SPR setup

Based on the measure of the plasmon extinction, many variations can be proposed depending on the aspect that needs to be stressed: rigorous illustrations of electromagnetism, qualitative effects or even demonstrative experiments for non-specialist audience.

### 5.1. SPR extinction measured with a convergent beam

Instead of recording the reflected intensity point by point as presented in section 4, the curve can be recorded in one shot by either using a CCD array or a digital camera. In this method, the progressive change of the incidence angle achieved by adjusting the rotation stage described in section 4 is replaced by impinging a convergent beam on the gold film. All the angles are ‘contained’ in this convergent beam so that after reflection, the plasmon extinction can be visualized directly on a screen. The initial setup is slightly modified in order to expand the He–Ne laser beam and create a large cylindrical beam as can be seen in figure 6. The beam is focused by a 100 mm convergent lens near the gold film, and the reflected beam can be directly observed on the screen. A semitransparent screen is used in figure 6 because it makes the photography of the resulting plasmon extinction easier. This extinction appears now as a black vertical line slightly bowed. By changing the polarization of the incident light from  $p$  to  $s$ , this black line vanishes which is a proof that the plasmon is actually observed. Photography of the plasmon image should be made with low sensitivity: usually, automatic exposure modes of digital cameras will yield saturated pixels. The picture in the inset of figure 6 has been taken with an underexposure of 2.0 diaphragm units. The picture is analysed by ImageJ [10], and the intensity profile following the dashed white line represented in the inset of figure 6 can be plotted. Such a plot reproduces the plasmon extinction curve. The curve is normalized by the intensity profile of the beam itself obtained by taking a second picture after having changed the polarization of light from  $p$  to  $s$  and keeping all the settings of the camera unchanged. The resulting curve is the curve (b) in figure 5. To set the horizontal angular scale in this measurement, the numerical aperture of the beam is calculated (half of the ratio of the beam diameter over the focal length) and is multiplied by a factor of 2 due to the reflection on the gold film. The shape of the plasmon extinction is well reproduced but the curve exhibits many fluctuations due to diffraction patterns originating from the defects of the various optical elements. Moreover, the response of the sensors of a digital camera is probably not linear.

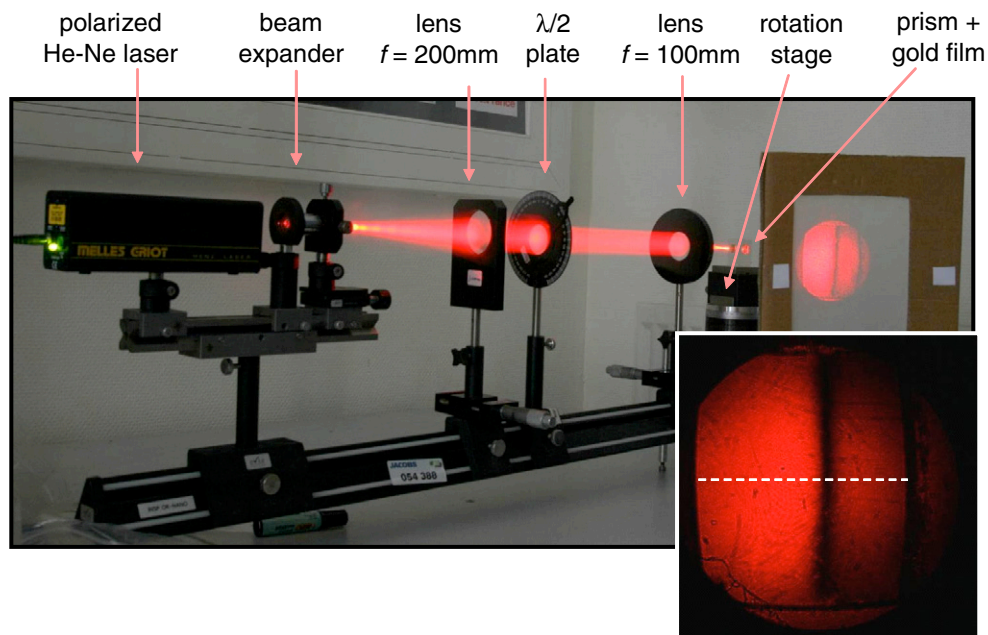


**Figure 6.** Optical setup for directly measuring the plasmon extinction. A digital photograph of the divergent beam reflected by the gold thin film is shown and the intensity of light is digitized along the dashed line. The profile is normalized to the intensity profile obtained with  $s$ -polarization. The resulting plasmon curve is given in figure 5(b).

This experiment is a good way to illustrate the sensitivity of the SPR. In the case of any perturbation of the outer surface of gold, the plasmon extinction line is displaced. For example, blowing on the golden film is sufficient to alter the black plasmon extinction line.

### 5.2. Dependence of the SPR extinction on the excitation wavelength

The SPR strongly depends on the excitation wavelength through the dependence of the dielectric functions (see equation (10)). The direct imaging of the plasmon extinction line described in the previous section is a practical way to illustrate the dependence of the SPR on the wavelength. To that end, the He-Ne laser is replaced by a white lamp equipped with a set of narrow-band interferential filters ( $\Delta\lambda = 3\text{ nm}$ ) placed on a filter wheel. The images obtained at 633 nm (red), 589 nm (yellow) and 546 nm (green) are presented in figure 7 along with the corresponding extinction curves obtained by the same process as before (section 5.1). As the wavelength decreases, the extinction angle increases in agreement with the plot of the dispersion relation (figure 2). The intersection of the light line in glass with the SPR dispersion curves is possible if the slope  $c/n \sin \theta$  decreases which is the case for increasing angles. For example, the plasmon extinction is detected at an internal angle of  $41.8^\circ$ ,  $42.3^\circ$  and  $43.1^\circ$  for wavelengths of 633, 589 and 546 nm respectively.

But the most striking result is the damping of the SPR when the wavelength shifts from red to green. This effect is clearly illustrated by the curves of figure 7 where the resonance is all the less pronounced as the wavelength decreases. With a blue interferential filter (435 nm) the extinction is not visible anymore (result not presented here). The damping of the resonance is a result of the coupling of the plasmon resonance with the interband transitions

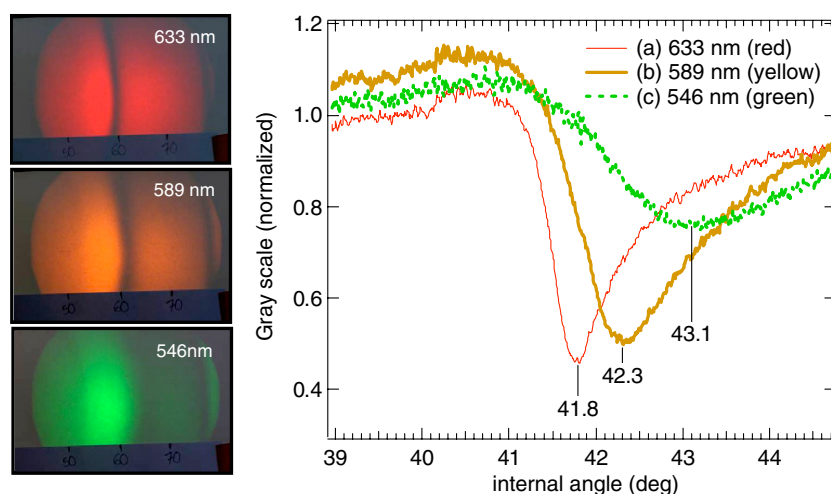


**Figure 7.** The plasmon profile obtained with different wavelengths. The three photos of the left panel show the reflected beam exhibiting a black stripe due to the plasmon extinction. The light source is a white light filtered with narrow-band interferential filters. The plasmon shifts from  $41.8^\circ$  up to  $43.1^\circ$  as the wavelength decreases. The most striking effect is the damping of the SPR due to the coupling with the interband transitions of gold.

of gold whose uptake is situated at 2.65 eV (468 nm). Since the three wavelengths presented in this paper are situated at energies below the interband transitions, they only partially couple with them and this explains why the damping is all the more weak as the wavelength goes away from 468 nm. Therefore, if sharp plasmon resonances are required, it is preferable to use near infrared light. In some commercial SPR setups, this approach has been developed to improve the sensibility of SPR sensing. Near-infrared laser diodes are used instead of the classical He–Ne laser.

Note that with a cylindrical beam (remove the  $f = 100$  mm focusing lens) and white light (remove the interferential filters), the setup produces a reflected beam that exhibits nice colourations corresponding to the complementary colour of the plasmon wave being excited. This can be used as a visual demonstration of the phenomena occurring at a nanometre scale for non-scientific audiences.

### 5.3. Towards biosensing

The most widespread use of the SPR is found in biochemistry, following the pioneering work of the Biacore company, which started to sell its first apparatus in 1991. The idea of biosensing is simple. Since SP waves have a spatial extension of 100 nm or so away from the gold surface, with great sensitivity to any optical index change, this provides a way of specifically sensing the vicinity of the gold surface. If a molecule adsorbs on the surface, the index  $n_2$  ( $n_2^2 = \epsilon_2$ ) of relation (10) is replaced by the local index of the molecular monolayer and its value is increased so that the right member also increases.  $\theta_{\text{int}}$  given in this equation needs to be increased as well, and the extinction is therefore slightly shifted to a higher angle. The principle of the sensor is to monitor the evolution versus time of the reflected intensity at a well-chosen angle. These ideas can be tested with the setup discussed in section 4 (use a He–Ne laser without beam expander). For example, in figure 5, the adjustment of the rotation stage such that the

internal angle is  $41.4^\circ$  (angle marked A in the figure) would be a good choice. Any positive changes in the index will be detected as an increase in the reflected intensity. If the signal of the photodiode is monitored with an oscilloscope, this can be illustrated simply by blowing on the gold film. However, the reactions of interest occur in liquid solutions so that the index of the medium surrounding the gold film is around  $n_2 = 1.33$  instead of 1. As a consequence, the plasmon extinction is measured at an internal angle of  $62^\circ$  and the gold film has to be inserted in a flow cell.

The setup presented here is somehow too elemental to allow reproducible experiments for biological interaction. It is not suited to accepting a flow cell although this could be implemented. Moreover a typical biological interaction induces a reflectivity change of an order of magnitude of 1% which corresponds more or less to the signal-to-noise ratio of our setup [11]. And finally, the knowledge for setting up a careful biological test of a specific interaction between, for example, a protein and an antibody is part of biology classes. This is not the aim of the present setup. Laboratory experiments have been proposed to teach the SPR to biologists, using commercial apparatus [12]. Many ideas for developing this experiment can be found in the research field and especially in the field of biophysics [13–15]. The development of a more sensitive setup is described by Lavine and coworkers [9].

## 6. Conclusion

The present paper describes a set of experiments to help understand the fundamental properties of the surface plasmon resonance. The main experiment is the excitation of the plasmon resonance with a He–Ne laser in the Kretschmann configuration where the gold active film is placed on a glass prism. The angular position of the plasmon extinction is accurately measured and compared to the theoretical prediction. This first experiment is an efficient way to introduce senior students to the concepts of plasmonics. Three other experiments based on this plasmon extinction are also described and the dependence of the resonance on the excitation wavelength is discussed. It is shown that the coupling of the surface plasmon wave with the interband transitions of gold leads to strong damping of the resonance when the wavelength shifts from red to blue. The setup is easy to adjust and handle and provides a good illustration of the electromagnetic principles at play in the SPR. More details regarding the setup and the commercial equipment being developed can be requested from the author.

## Acknowledgments

The authors are indebted to the senior students who have worked with the setup and helped in its preliminary testing and improvement. Financial support from C’Nano IdF is acknowledged and we are grateful to the *Service d’Optique* of the University Pierre et Marie Curie and its helpful technicians, C Sajas, L Delbès and J P Ferreira. We also thank C Frydman from HORIBA-Jobin Yvon for helpful discussions and ideas to further develop the experiment.

## Appendix. Complete derivation of the plasmon dispersion relation

We give here the detailed calculation to derive the SP dispersion relation [3, 4].

We consider a  $p$ -polarized electric field at the interface of medium 1 (metal) and medium 2 (dielectric) as depicted in figure 1 in the text.

In medium 1 (resp. medium 2), of dielectric function  $\varepsilon_1$  (resp.  $\varepsilon_2$ ), the electric field is written as

$$\vec{E}_1 = \begin{bmatrix} E_{1x} \\ 0 \\ E_{1z} \end{bmatrix} e^{i(k_{1x}x - \omega t)} \cdot e^{ik_{1z}z} \quad \left( \text{resp. } \vec{E}_2 = \begin{bmatrix} E_{2x} \\ 0 \\ E_{2z} \end{bmatrix} e^{i(k_{2x}x - \omega t)} \cdot e^{ik_{2z}z} \right).$$

At the interface, both fields obey the boundary conditions for the components of the electric field parallel and perpendicular to the interface. The component of the electric field parallel to the interface is continuous at any point of the interface:

$$\forall x \in \text{interface}, \forall t, E_{1x} \cdot e^{i(k_{1x}x - \omega t)} = E_{2x} \cdot e^{i(k_{2x}x - \omega t)}. \quad (\text{A.1})$$

The fact that this relation has to be fulfilled at any point of the interface implies that the component of the wavevector parallel to the interface is equal on both sides of the interface  $k_{1x} = k_{2x}$  which is noted as  $k_x$  in the following. Relation (A.1) also drives to

$$E_{1x} = E_{2x}. \quad (\text{A.2})$$

The component of the electric field perpendicular to the interface is not continuous, unlike the displacement vector which reads

$$\forall x \in \text{interface}, \forall t, \varepsilon_1 E_{1z} \cdot e^{i(k_{1x}x - \omega t)} = \varepsilon_2 E_{2z} \cdot e^{i(k_{2x}x - \omega t)}$$

which leads to

$$\varepsilon_1 E_{1z} = \varepsilon_2 E_{2z}. \quad (\text{A.3})$$

Moreover, since both media are free of sources, the Maxwell equation  $\text{div} \vec{D} = 0$  leads to

$$k_x E_{1x} + k_{1z} E_{1z} = 0 \quad (\text{A.4})$$

$$k_x E_{2x} + k_{2z} E_{2z} = 0. \quad (\text{A.5})$$

Equations (A.2)–(A.5) form a set of four equations with four unknown field components. We seek to express  $k_x$  as a function of the dielectric functions.

The combination of equations (A.2), (A.3) and (A.5) easily leads to

$$\varepsilon_2 k_x E_{1x} + \varepsilon_1 k_{2z} E_{1z} = 0. \quad (\text{A.6})$$

The coupled equations (A.4) and (A.6) lead to nontrivial solutions if the corresponding determinant vanishes:  $\varepsilon_1 k_x k_{2z} - \varepsilon_2 k_x k_{1z} = 0$ . This latter equation has two solutions: either  $k_x = 0$  which does not correspond to a wave travelling along the interface, or the solution

$$\varepsilon_1 k_{2z} - \varepsilon_2 k_{1z} = 0. \quad (\text{A.7})$$

In this latter relation and using equation (3) for both sides of the boundary, the components  $k_{1z}$  and  $k_{2z}$  are expressed as functions of  $k_x$ . This leads to the relation  $\varepsilon_1^2 (\varepsilon_2 \frac{\omega^2}{c^2} - k_x^2) = \varepsilon_2^2 (\varepsilon_1 \frac{\omega^2}{c^2} - k_x^2)$  which simplifies to

$$k_x^2 = \frac{\omega}{c^2} \cdot \frac{\varepsilon_1 \varepsilon_2}{\varepsilon_1 + \varepsilon_2},$$

which is the dispersion relation of the surface plasmon wave (7) given in the text.

The combination of this dispersion equation with equation (3) gives access to the component of the wavevector normal to the interface  $k_{1z}$ , which is equation (8) discussed in section 2.3:

$$k_{1z}^2 = \frac{\omega^2}{c^2} \cdot \frac{\varepsilon_1^2(\omega)}{\varepsilon_1(\omega) + \varepsilon_2(\omega)}.$$

The relation for  $k_{2z}$  is obtained similarly:  $k_{2z}^2 = \frac{\omega^2}{c^2} \cdot \frac{\varepsilon_2^2(\omega)}{\varepsilon_1(\omega) + \varepsilon_2(\omega)}.$



## References

- [1] Otto A 1968 Excitation of nonradiative surface plasma waves in silver by method of frustrated total reflection *Z. Phys.* **216** 398
- [2] Kretschmann E 1971 Die Bestimmung optischer Konstanten von Metallen durch Anregung von Oberflächenplasmaschwingungen *Z. Phys. A* **241** 313–24
- [3] Novotny L and Hecht B 2006 *Principles of Nano-Optics* (Cambridge: Cambridge University Press)
- [4] Raether H 1986 *Surface Plasmons on Smooth and Rough Surfaces and on Gratings* (Berlin: Springer)
- [5] Kittel C 2004 *Introduction to Solid State Physics* (New York: Wiley)
- [6] Arwin H 2007 Dielectric function of gold measured by ellipsometry, private communication, University of Linköping, Sweden
- [7] Etchegoin P G, Le Ru E C and Meyer M 2006 An analytic model for the optical properties of gold *J. Chem. Phys.* **125** 164705
- [8] Johnson P B and Christy R W 1972 Optical constants of the noble metals *Phys. Rev. B* **6** 4370
- [9] Lavine B K, Westover D J, Oxenford L, Midankar N and Kaval N 2007 Construction of an inexpensive surface plasmon resonance instrument for use in teaching and research *Microchem. J.* **86** 147–55
- [10] ImageJ 2010 ImageJ is a software providing image processing and analysis; it can be freely downloaded from <http://rsbweb.nih.gov/ij/> (National Institute of Health)
- [11] Uzun L, Say R, Ünal S and Denizli A 2009 Production of surface plasmon resonance based assay kit for hepatitis diagnosis *Biosens. Bioelectron.* **24** 2878–84
- [12] Kausaite A, van Dijk M, Castrop J, Ramanaviciene A, Baltrus J P, Acaite J and Ramanavicius A 2007 Surface plasmon resonance label-free monitoring of antibody antigen interactions in real time *Biochem. Mol. Biol. Educ.* **35** 57–63
- [13] Jung L S, Campbell C T, Chinowsky T M, Ma M N and Yee S S 1998 Quantitative interpretation of the response of surface plasmon resonance sensors to adsorbed films *Langmuir* **14** 5636–48
- [14] Homola J, Yee S S and Gauglitz G 1999 Surface plasmon resonance sensors: review *Sensors Actuator B* **54** 3–15
- [15] Brockman J M, Nelson B P and Corn R M 2000 Surface plasmon resonance imaging measurements of ultrathin organic films *Annu. Rev. Phys. Chem.* **51** 41–63